Analyst

Accepted Manuscript

ROYAL SOCIETY OF CHEMISTRY

www.rsc.org/analyst

Fenton reaction-mediated fluorescence quenching of N-acetyl-L-cysteine-protected gold nanoclusters: analytical applications for hydrogen peroxide, glucose, and catalase detection

Hao-Hua Deng,[a,b] Gang-Wei Wu,[a,c] Dong He,[a,b] Hua-Ping Peng,[a,b] Ai-Lin Liu,[a,b] Xing-Hua Xia,[d] Wei Chen*[a,b]

[a] Department of Pharmaceutical Analysis, Fujian Medical University, Fuzhou 350004, China

[b] Higher Educational Key Laboratory for Nano Biomedical Technology of Fujian Province, Fujian Medical Univeristy, Fuzhou 350004, China

[c] Department of Pharmacy, Fujian Provincial Hospital, Fuzhou 350001, China

[d] State Key Laboratory of Analytical Chemistry for Life Science, School of Chemistry and Chemical Engineering, Nanjing University, Nanjing 210093, China.

* Corresponding author. Tel./fax: +86 591 22862016.

E-mail address: chenandhu@163.com (W. Chen).

Hao-Hua Deng and Gang-Wei Wu contributed equally to this work.

Abstract

Given the importance of hydrogen peroxide (H_2O_2) in many biological processes and its wide application in various industries, the demand for sensitive, accurate, and economical H_2O_2 sensors is high. In this study, we used Fenton reaction-stimulated fluorescence quenching of N-acetyl-L-cysteine-protected gold nanoclusters (NAC-AuNCs) as a reporter system for the determination of H_2O_2. After experimental conditions were optimized, the sensing platform enabled the analysis of H_2O_2 with a limit of detection (LOD) as low as 0.027 μM. As the glucose oxidase cascade leads to the generation of H_2O_2 and catalase catalyzes the decomposition of H_2O_2, these two biocatalytic procedures could be probed by the Fenton reaction-mediated quenching of NAC-AuNCs. The LOD for glucose was found to be 0.18 μM, and the linear range

was 0.39–27.22 μM. The LOD for catalase was 0.002 U/mL, and the linear range was 0.01–0.3 U/mL. Moreover, the proposed sensing methods were successfully applied for human serum glucose detection and noninvasive determination of catalase activity in human saliva, demonstrating their great potential for practical applications.

Introduction

Hydrogen peroxide (H_2O_2) is a vitally important chemical reagent and is widely used in various fields including the textile industry, food processing, clinical chemistry, pharmaceutical research, and environmental protection. In addition, H_2O_2 plays a significant role in various cellular biochemical processes and has been confirmed to be a secondary messenger.[1] Furthermore, it is the main product of reactions catalyzed by numerous O_2-dependent oxidase enzymes (e.g., glucose oxidase, cholesterol oxidase, lactate oxidase, choline oxidase, xanthine oxidase, and monoamine oxidase) and also is a substrate for enzymes such as horseradish peroxidase (HRP) and catalase. Therefore, the construction of highly sensitive, accurate, and economical H_2O_2 sensors continues to be extensively investigated. Until date, several analytical approaches such as spectrophotometry,[2] fluorometry,[3-7] electrochemistry,[8] chemiluminescence,[9] resonance light scattering assay,[10] and chromatography have been used for H_2O_2 detection.[11] Among these, fluorescence detection has many advantages over the other techniques, including high spatial and temporal resolution, sensitivity, specificity, rapidity, and simplicity. Although a variety of fluorescent sensors have been dedicated to the determination of H_2O_2,[3-7] their practical deployment is limited by their relatively poor photostability, biotoxicity, spontaneous autoxidation, and high cost. Therefore, developing new probes with improved features is still a challenging and fascinating area in chemistry.

In the past decades, nanomaterials, particularly metal nanostructured materials, have been widely used in biomedical research and the advances in nanoscale technologies contribute to the diagnosis, treatment, and prevention of diseases. Emerging as a novel type of nontoxic and harmless luminescent nanomaterials, gold nanoclusters (AuNCs) have recently gained a lot of attention in the fields of chemical,

physical, and biological sciences owing to their fantastic characteristics including remarkable water-solubility, facile synthesis, high colloidal stability, excellent biocompatibility, outstanding catalytic performance, and unusual photophysical properties.[12, 13] The fluorescent properties of AuNCs are dictated by the surrounding conditions as well as the size and surface ligands or scaffolds of the clusters, which allows them to be widely applied for the development of versatile sensors by various mechanisms such as metallophilic interactions, metal core surface deposition, metal core decomposition, cluster aggregation, incorporation of recognition moieties, and enzymatic reaction.[14] To date, various types of AuNC fluorescence probes have been developed for H_2O_2 determination. Jin et al. found that bovine serum albumin-protected AuNCs allow sensitive determination of H_2O_2 concentration and exhibit a linear response in the range of 1–100 μM.[15] Wen et al. reported that HRP-functionalized AuNCs can be obtained via a biomineralization process and can be employed as an efficient H_2O_2 detector within a linear range of 100 nM to 100 μM as the HRP enzyme remains active.[16] Recently, Chen et al. demonstrated that glutathione-capped gold nanoparticles can be etched by hydroxyl radical ($^{\bullet}OH$) generated from Fenton process and subsequently, form AuNCs through protein-induced the aggregation of Au(I)-thiolate complexes, showing great potential for H_2O_2 monitoring.[17]

In our previous study, we successfully synthesized AuNCs by using N-acetyl-L-cysteine (NAC) both as a reducing agent and as a stabilizing ligand. The resulting NAC-stabilized AuNCs (NAC-AuNCs) exhibited superior performance including good long-term stability and photostability, excellent salt and oxidation resistance, and red emission.[18] In this study, NAC-AuNCs were utilized as fluorescence probes for monitoring H_2O_2 in the presence of Fe^{2+}. Based on the determination of H_2O_2, we constructed an accurate, cost-effective, simple, and sensitive fluorescence sensor for quantitative analysis of glucose in human serum and catalase in human saliva.

Experimental Section

Materials and reagents

All chemicals and solvents were of analytical grade and commercially available. $HAuCl_4 \cdot 4H_2O$, N-acetyl-L-cysteine, 4-(2-hydroxyethyl)-1-piperazineethanesulfonic acid (HEPES), $FeCl_2 \cdot 4H_2O$, horseradish peroxidase (HRP) and glucose oxidase (GOx) were obtained from Aladdin Reagent Co., Ltd. (Shanghai, China). Catalase was purchased from Sigma-Aldrich (Shanghai, China). Glucose, H_2SO_4, H_2O_2, and NaOH were purchased from Sinopharm Chemical Reagent Co., Ltd. (Shanghai, China). Deionized water was used in all experiments.

Apparatus

The UV-vis absorption and photoluminescence spectra were recorded by using a UV-2450 UV-vis spectrophotometer (Shimadzu, Kyoto, Japan) and a Cary Eclipse fluorescence spectrophotometer (Agilent, Santa Clara, CA, USA), respectively. X-ray photoelectron spectroscopy (XPS) was performed using an ESCALAB 250XI X-ray photoelectron spectrometer (Thermo Fisher Scientific, Waltham, MA, USA) using monochromatic Al Kα radiation (1486.6 eV) for the analysis of the surface composition and chemical states of the product. Binding energy calibration was based on the binding energy of C 1s photoelectrons at 284.8 eV. All measurements were performed at room temperature under ambient conditions.

Preparation of NAC-AuNCs

All glassware used in the following procedures was cleaned in a bath of freshly prepared HNO_3-HCl (1:3, v/v) solution, rinsed thoroughly in water, and dried in air prior to use. AuNCs were synthesized by a blending procedure.[18] NaOH (0.6 mL, 0.5 M) and $HAuCl_4$ (0.4 mL, 20 mg/mL) were added to an aqueous solution of NAC (4 mL, 0.08 M). The mixture was incubated at 37 °C for 2.5 h, until the solution was completely colorless. The solution after synthesis was dialyzed for more than 24 h to remove all small-molecular impurity. The NAC-AuNCs solution was stored in the dark at 4 °C until use.

H_2O_2 sensing

H_2O_2 concentration was determined as follows: First, 25 μL H_2SO_4 solution was added to 200 μL HEPES solution (20 mM, pH = 7.4) containing different

concentrations of H_2O_2 to adjust the pH to 3.0. Then, 200 μL AuNCs solution and 25 μL Fe^{2+} (1.8 mM) solution were added to the solution and the mixed solution was incubated in a water bath at 25 °C for 10 min. Finally, the fluorescence spectrum of the solution was obtained by using a Cary Eclipse fluorescence spectrometer at an excitation wavelength of 355 nm.

Glucose sensing

The procedure for glucose determination was as follows: First, 25 μL 0.1 mg/mL GOx was added to 175 μL HEPES solution (20 mM, pH = 7.4) containing different concentrations of glucose and the solution was incubated in a water bath at 25 °C for 30 min. Then, 25 μL H_2SO_4 was added to adjust the pH to 3.0. After that, 200 μL AuNCs solution and 25 μL Fe^{2+} (1.8 mM) solution were added into the above solution and the mixed solution was incubated in a 25 °C bath for 10 min. Finally, the fluorescence spectrum of the solution was measured by using a Cary Eclipse fluorescence spectrometer at an excitation wavelength of 355 nm.

Glucose detection by oxidase endpoint method was carried out by adding 100 μL of 0.1 mg/mL GOx, 10 μL of 10 U/mL HRP, 20 μL of 16 mM 3,3',5,5'-tetramethylbenzidine (TMB), and 50 μL glucose of different concentrations into 320 μL of 20 mM HEPES solution (pH=7.4). The mixture was then incubated at 37 °C for 10 min. The resulting reaction solution was measured by using a Shimadzu UV-2450 spectrophotometer.

Catalase activity determination

Catalase activity was determined as follows: First, 25 μL solution containing different concentrations of catalase was added to 175 μL HEPES solution (20 mM, pH = 7.4) containing 25 μM H_2O_2 and the solution was incubated in a water bath at 25 °C for 90 min. Then, 25 μL H_2SO_4 was added to adjust the pH to 3.0. After that, 200 μL AuNCs and 25 μL Fe^{2+} (1.8 mM) solutions were added to the solution and the mixed solution was incubated in a water bath at 25 °C for 10 min. Finally, the fluorescence spectrum of the solution was measured by using a Cary Eclipse fluorescence spectrometer under the excitation wavelength of 355 nm.

Catalase activity detection by UV method was carried out by adding 50 μL of 0.1

M H_2O_2 and 200 μL catalase solution into 3.75 mL HEPES solution (20 mM, pH = 7.4). The decrease in H_2O_2 absorbency at 240 nm was followed during 5 min at 25 °C according to Góth.[19]

Human serum and saliva samples detection

For glucose detection in serum, the samples were pretreated by ultra-filtration to eliminate possible interference by proteins. The pretreated samples were diluted in HEPES solution (20 mM, pH = 7.4) and glucose concentrations were determined as described above. For determination of catalase activity, human saliva samples centrifuged at 6000 rpm for 10 min. The pretreated samples were diluted in HEPES solution (20 mM, pH = 7.4) and catalase activity was determined as described above.

Results and discussion

Strategy and proof of concept of the NAC-AuNCs sensor

We developed a novel analytical sensor to detect H_2O_2 based on NAC-AuNCs. First, we investigated the changes in fluorescence spectra of the NAC-AuNCs in the presence of H_2O_2. As indicated in Fig. 1A-b, the fluorescence intensity of NAC-AuNC solution containing 25 μM H_2O_2 showed no obvious change as compared to NAC-AuNC solution alone (Fig. 1A-a), implying that the NAC-AuNCs are insensitive to H_2O_2. Next, we tested the effect of Fe^{2+} on the fluorescence intensity of the NAC-AuNCs. The results showed that the fluorescence of the NAC-AuNCs changed only inconspicuously in the presence of 100 μM Fe^{2+} (Fig. 1A-c). However, when H_2O_2 (25 μM) and Fe^{2+} (100 μM) were simultaneously present in the NAC-AuNC solution, the fluorescence of the NAC-AuNCs decreased dramatically (Fig. 1A-d). These results demonstrated that both H_2O_2 and Fe^{2+} are needed for quenching of the NAC-AuNC fluorescence.

H_2O_2 is reduced by Fe^{2+} to form $^{\bullet}OH$, which is known as the Fenton reaction. The $^{\bullet}OH$ radical has higher oxidizing ability than does H_2O_2. Therefore, it is possible that the $^{\bullet}OH$ generated from the Fenton reaction caused the fluorescence quenching of NAC-AuNCs. To examine this, thiourea, an effective $^{\bullet}OH$ scavenger,[20] was added to the NAC-AuNC-based sensing system. The results showed that the fluorescence

quenching of the NAC-AuNCs was greatly suppressed when 300 μM thiourea was introduced (Fig. 1A-e), revealing that $^{\bullet}OH$ indeed plays an important role in the fluorescence quenching of NAC-AuNCs. To elucidate the mechanism of $^{\bullet}OH$-induced fluorescence quenching, we used XPS to analyze the oxidation state of the NAC-AuNCs. As shown in Fig. 1B, the NAC-AuNCs showed an Au ($4f_{7/2}$) peak at 84.57 eV, which suggests that Au(0) and Au(I) coexist on the surface of NAC-AuNCs. The best fit of the data illustrated that the percentage of Au(0) and Au(I) was 42% and 58%, respectively. When the NAC-AuNCs were subjected to the Fenton reaction, the Au ($4f_{7/2}$) peak shifted to 84.75 eV, signifying that only Au(I) was present on the surface of final products.[17] This result was in agreement with previously reported results,[21-23] and the fluorescence quenching effect was ascribed to the strong oxidative power of $^{\bullet}OH$, which oxidizes the Au^0 in AuNCs to Au^+. Scheme 1 depicts the principle of the NAC-AuNCs-based fluorescence sensor for H_2O_2.

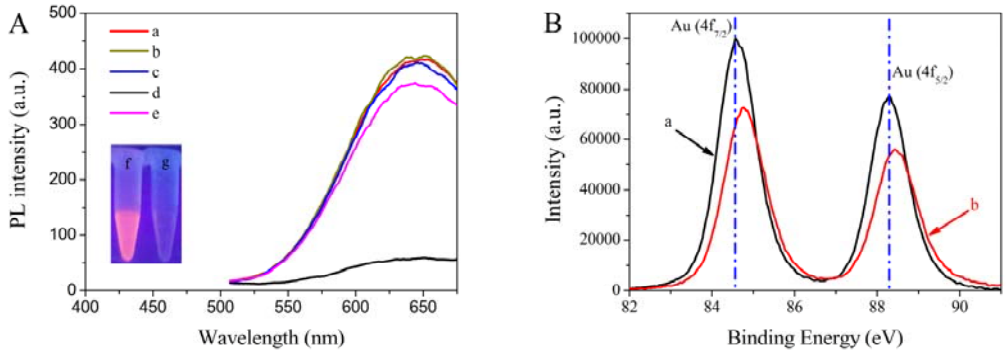

Fig. 1 (A) Fluorescence intensity of (a) AuNCs, (b) AuNCs + 25 μM H_2O_2, (c) AuNCs + 100 μM Fe^{2+}, (d) AuNCs + 25 μM H_2O_2 + 100 μM Fe^{2+}, and (e) AuNCs + 25 μM H_2O_2 + 100 μM Fe^{2+} + 300 μM thiourea. Inset: Photograph of (f) AuNCs and (g) AuNCs + 25 μM H_2O_2 + 100 μM Fe^{2+} under UV irradiation. (B) XPS spectra of AuNCs alone (a) and of AuNCs in the presence of 100 μM H_2O_2 and 100 μM Fe^{2+} (b).

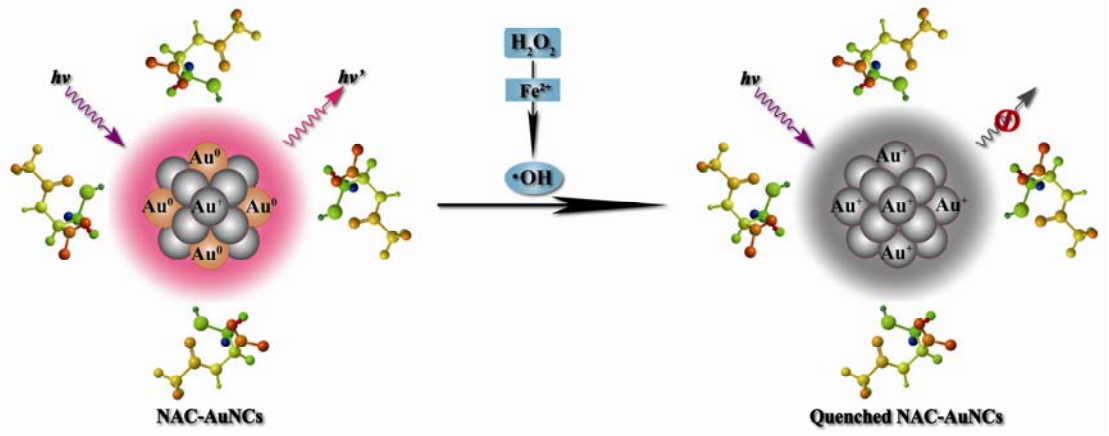

Scheme 1 Schematic representation of the Fenton reaction-mediated NAC-AuNCs fluorescence quenching.

Detection of H_2O_2 based on NAC-AuNCs and the Fenton reaction

Next, we optimized the NAC-AuNCs-based sensor for successful determination of H_2O_2; the effects of operational parameters including solution pH, Fe^{2+} concentration, and reaction time were investigated. We used the fluorescence intensity change ΔF ($\Delta F = F_0 - F_t$, where F_0 and F_t are the fluorescence intensities at 650 nm of the NAC-AuNCs before and after the reaction, respectively) as a signal for H_2O_2 detection.

The solution pH is a vital factor influencing the Fenton reaction, which usually requires low pH because Fe^{3+} precipitates as hydroxide inhibiting the recycling of Fe^{2+}/Fe^{3+} at higher pH.[24] Therefore, we first estimated the effect of solution pH on the ΔF values. Fig. S1A shows that ΔF initially increased with increasing pH, reached a maximum at pH 3.0, and then decreased at pH >3.0. Based on these results, a solution pH of 3.0 was used in subsequent experiments. Because Fe^{2+} is an indispensable factor affecting the generating of •OH, the influence of the Fe^{2+} concentration on ΔF was explored. The results are shown in Fig. S1B. ΔF gradually increased with increasing concentration of Fe^{2+} and reached a plateau above 100 μM Fe^{2+}. To avoid the formation of iron sludge,[25] an Fe^{2+} concentration of 100 μM was used in further assays. In addition, Fig. S1C illustrates that the fluorescence intensity became nearly constant after 10 min. Therefore, the reaction time was set at 10 min.

Under the optimal conditions (solution pH 3.0, 100 μM Fe^{2+}, and reaction time of

10 min), the calibration plot for the determination of H_2O_2 was obtained by establishing a linear correlation between ΔF and the concentration of H_2O_2 (Fig. 2). Fig. 2B shows that ΔF was linearly correlated with the concentration of H_2O_2 in the range of 0.04 to 6.66 μM with a correlation coefficient of 0.993. The limit of detection (LOD) was as low as 0.027 μM (at S/N = 3), which was superior to that of previously reported methods for H_2O_2 detection.[16, 26-30] The relative standard deviation (RSD) was 2.2% for 4.44 μM H_2O_2 (n = 12). Remarkably, no obvious quenching of the fluorescence intensity of NAC-AuNCs was observed after their exposure to other typical reactive oxygen species (ROS) such as $O_2^{\bullet}$, $^1O_2$, $ClO^{\bullet}$, and $ONOO^{\bullet}$, revealed that the present probe had high selectivity for H_2O_2 determination (Fig. S2).

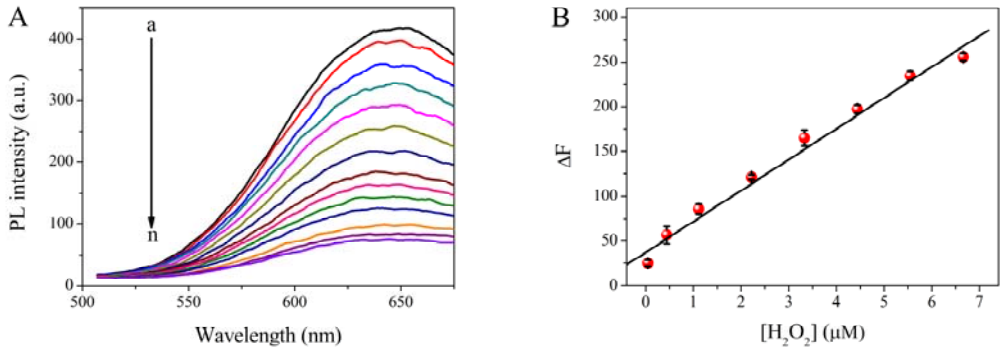

Fig. 2 (A) Quenching of AuNC emission by different concentrations of H_2O_2 (from top to bottom: 0, 0.044, 0.44, 1.11, 2.22, 3.33, 4.44, 5.55, 6.66, 7.77, 8.88, 9.99, 11.11, and 13.33 μM). (B) Correlation between the change in the fluorescence intensity of the NAC-AuNC solution (ΔF) and the H_2O_2 concentration.

Analytical application of the NAC-AuNC sensor for the detection of glucose

Glucose is a main source of energy for living cells and plays a critical role in metabolism. Abnormal blood or urine glucose levels are commonly used as clinical indicators of diabetes or hypoglycemia. Hence, accurate and rapid determination of glucose is of vital importance in clinical diagnostics and the food industry. Enzymatic glucose biosensors have been intensively applied in electrochemical and optical detection of glucose due to their advantages in terms of reliability, sensitivity, and selectivity. In this regard, GOx, which catalyzes the oxidation of glucose in the presence of O_2 to yield H_2O_2, is the most popular enzyme for highly specific and

sensitive monitoring of glucose. As H_2O_2 is the product of glucose oxidation, glucose can be detected based on the Fenton reaction-mediated fluorescence quenching of NAC-AuNCs through cascade reactions using GOx. In this study, a two-step reaction was carried out: First, H_2O_2 was formed by GOx-catalyzed oxidation of glucose (pH 7.4) and the solution pH was adjusted to 3.0. Then, NAC-AuNCs and Fe^{2+} were added to the solution to initiate the Fenton reaction and the fluorescence intensity was measured. Different concentrations of glucose were used to evaluate the sensitivity of the novel glucose-sensing platform. The calibration curve was found to be linear in the concentration range from 0.39 to 27.22 μM (Fig. 3A). The correlation coefficient was 0.992, and the RSD for twelve repeated measurements of 7.78 μM glucose was 1.9%. The LOD was 0.18 μM (S/N = 3), which was much lower than the average concentration of glucose in serum. In addition, the LOD of our sensor was lower than that reported for methods utilizing metal nanoclusters,[15, 31-33] semiconductor quantum dots,[34-36] carbon dots,[37, 38] and grapheme oxide dots as fluorescence probes.[39] The control experiment showed that glucose (5 mM) or GOx (1 mg/mL) did not interfere with the fluorescence of the NAC-AuNCs, proving that the quenching of the NAC-AuNC fluorescence was caused by the $^{\bullet}OH$ generated from the Fenton reaction.

Selectivity is another important factor in the performance of sensors. Therefore, we tested the selectivity of our novel platform by using lactose, maltose, and fructose. No obvious signals were detected for these control samples, which dues to the high substrate specificity of GOx (Fig. 3B). Hence, a novel "turn-off" assay based on the Fenton reaction-stimulated quenching of the NAC-AuNCs and GOx-catalyzed oxidation of glucose could be successfully fabricated for the detection of glucose.

The high sensitivity and outstanding specificity of the sensing system suggest that it could be used to detect glucose in clinical samples. Table 1 lists the glucose content determined in three human serum samples using both our established method and the glucose oxidase endpoint method. A *t*-test and an F-test performed at a 95% confidence level demonstrated that the results obtained by the two methods did not significantly differ. The feasibility of our method was further validated by standard addition experiments. The recoveries of glucose from the three serum samples ranged

from 100.6% to 105.2%. Taken together, our results demonstrated that the biosensor is suitable for glucose detection in clinical samples.

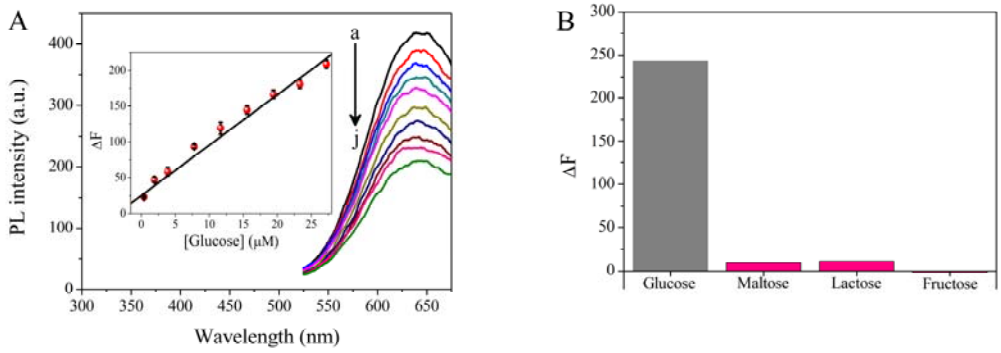

Fig. 3 (A) Emission spectra of NAC-AuNCs in the presence of varying concentrations of glucose. a–j: 0, 0.39, 1.94, 3.89, 7.78, 11.67, 15.56, 19.44, 23.33, 27.22 μM. Inset: correlation between the change of F_{650} (ΔF) of the NAC-AuNC solution and glucose concentration. (B) The ΔF of the glucose sensing system in the presence of glucose (40 μM), maltose (40 μM), lactose (400 μM), and fructose (400 μM).

Table 1 Analysis of glucose in human serum samples

Samples	Proposed method (mM, mean ± SD, n = 3)	Glucose oxidase endpoint method (mM, mean ± SD, n = 3)	F-test	*t*-test
1	3.95±0.10	3.91±0.12	1.44	0.44
2	4.14±0.19	3.95±0.14	1.84	1.54
3	6.07±0.40	6.18±0.25	2.56	0.40

$F_{0.05,\,2,\,2} = 19.00$, $t_{0.05,\,4} = 2.776$

Analytical application of the NAC-AuNC sensor for the detection of catalase activity

Catalase (EC 1.11.1.6) is an antioxidant enzyme found in nearly all living organisms, which contains four porphyrin heme (iron) groups per molecule. It catalyzes the decomposition of H_2O_2 to O_2 and H_2O and protects the cells and tissues from oxidative damage by H_2O_2. An increase in catalase activity is often related to the

emergence of diseases such as hemolytic and acute pancreatitis.[40] In addition, catalase is commonly used in the food, textile, and aesthetics industries. Therefore, accurate quantitative determination of catalase activity is of paramount importance. To the best of our knowledge, detection of catalase by using AuNCs has not been reported until date. Similar to the glucose detection, the assay for catalase activity determination was conducted in two steps: catalase-catalyzed H_2O_2 decomposition followed by the Fenton reaction. Different concentrations of catalase were tested and the ΔF values were plotted against the concentrations. The ΔF was linearly related to the catalase concentration in the range from 0.01 to 0.3 U/mL (r = 0.996) (Fig. 4A). The RSD was 2.7% for the detection of 0.05 U/mL catalase (n = 12), and the LOD was 0.002 U/mL (S/N = 3). A control experiment showed that catalase (10 U/mL) did not interfere with the fluorescence of the NAC-AuNCs.

Next, we tested the anti-interference ability of our platform for catalase sensing. As displayed in Fig. 4B, the interference of foreign substances was negligible. The results proved that a sensitive and selective "turn-on" catalase biosensor based on the Fenton reaction-stimulated quenching of the NAC-AuNCs could be developed in a facile manner.

Finally, we examined the applicability and feasibility of our novel approach for catalase activity detection in real samples. Catalase activity was determined in human saliva samples by using both the proposed method and the conventional UV method.[19] A *t*-test and an F-test performed at a 95% confidence level indicated that the results obtained by the two methods did not significantly differ (Table 2). Moreover, the recoveries of catalase from the three human saliva samples ranged from 93.5% to 102.2%. Taken together, the results indicated that the method presented here is suitable for the analysis of catalase in biological samples.

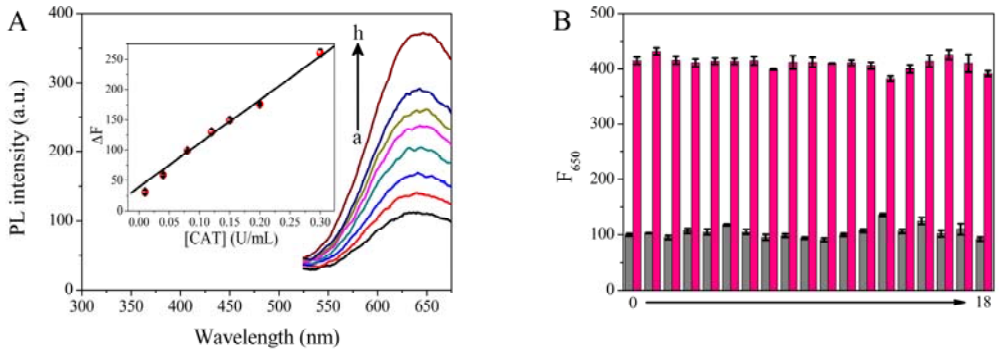

Fig. 4 (A) Emission spectra of NAC-AuNCs in the presence of varying concentrations of catalase. a–h: 0, 0.01, 0.04, 0.08, 0.12, 0.15, 0.2, 0.3 U/mL. Inset: linear relationship between the change of F_{650} (ΔF) and the enzyme activity of catalase. (B) Fluorescence intensity of catalase sensing system in the presence of different molecules. (0) NAC-AuNCs alone (gray) and after addition of catalase (pink); (1-18) NAC-AuNCs in presence of $CaCl_2$, $ZnSO_4$, KCl, $NaHCO_3$, NaH_2PO_4, $MgCl_2$, glucose, lactate, creatine, creatinine, urea, acetylcholine, glutathione, catechol-O-methyl transferase, urease, carboxylesterase, acetylcholinesterase, lysozyme (gray) and after the addition of catalase (pink). The concentrations of catalase, catechol-O-methyl transferase, urease, carboxylesterase, acetylcholinesterase and lysozyme are all 0.5 U/mL, and that of other interferents is 100 μM.

Table 2 Analysis of catalase activity in human saliva samples

Samples	Proposed method (U/mL, mean ± SD, n = 3)	UV method (U/mL, mean ± SD, n = 3)	F-test	*t*-test
1	11.86±0.92	13.01±0.43	4.58	1.96
2	16.06±0.86	14.67±1.14	1.76	1.69
3	18.87±0.76	18.12±0.29	6.87	1.60

$F_{0.05,2,2} = 19.00$, $t_{0.05,4} = 2.776$

Conclusions

In the present study, we fabricated a sensitive sensor for H_2O_2 detection through the

Fenton reaction-stimulated quenching of NAC-AuNCs. The novel H_2O_2-sensing platform was successfully implemented to construct a "turn-off" biosensor for glucose (by following H_2O_2 produced by GOx cascade) and a "turn-on" biosensor for catalase (through the catalase-catalyzed decomposition of H_2O_2). To our knowledge, this is the first report on the detection of glucose and catalase based on AuNCs and the Fenton reaction. In addition, we validated the application of the proposed biosensor for serum glucose detection and noninvasive determination of catalase activity in saliva, which demonstrated its great prospect for use in diagnostics. Since multitudinous O_2-dependent oxidase enzymes yield H_2O_2, the approach may also be applied to monitor other substrates and enzyme activities. The versatile strategy demonstrated here will open up new potential applications of metal nanoclusters for the development of fluorescence chemo/biosensors.

Acknowledgments

The authors gratefully acknowledge the financial support of the National Natural Science Foundation of China (21175023), the Program for New Century Excellent Talents in University (NCET-12-0618), and the Medical Elite Cultivation Program of Fujian Province (2013-ZQN-ZD-25).

References

[1] G. Georgiou and L. Masip, *Science*, 2003, **300**, 592-594.

[2] H. Wei and E. Wang, *Anal. Chem.*, 2008, **80**, 2250-2254.

[3] H. Chen, H. Yu, Y. Zhou and L. Wang, *Spectrochim. Acta A Mol. Biomol. Spectrosc.*, 2007, **67**, 683-686.

[4] N. Jie, J. Yang, X. Huang, R. Zhang and Z. Song, *Talanta*, 1995, **42**, 1575-1579.

[5] O.S. Wolfbeis, A. Dürkop, M. Wu and Z. Lin, *Angew. Chem. Int. Ed.*, 2002, **41**, 4495-4498.

[6] X. Shu, Y. Chen, H. Yuan, S. Gao and D. Xiao, *Anal. Chem.*, 2007, **79**, 3695-3702.

[7] K. Hirakawa, *Anal. Bioanal. Chem.*, 2006, **386**, 244-248.

[8] X. Zheng and Z. Guo, *Talanta*, 2000, **50**, 1157-1162.

[9] Y. Hu, Z. Zhang and C. Yang, *Anal. Chim. Acta*, 2007, **601**, 95-100.

[10] L. Shang, H. Chen, L. Deng and S. Dong, *Biosens. Bioelectron.*, 2008, **23**, 1180-1184.

[11] S. Oszwałdowski, R. Lipka and M. Jarosz, *Anal. Chim. Acta*, 2000, **421**, 35-43.

[12] L. Shang and G.U. Nienhaus, *Mater. Today*, 2013, **16**, 58-66.

[13] L. Shang, S. Dong and G.U. Nienhaus, *Nano Today*, 2011, **6**, 401-418.

[14] X. Yuan, Z. Luo, Y. Yu, Q. Yao and J. Xie, *Chem.-Asian J.*, 2013, **8**, 858-871.

[15] L. Jin, L. Shang, S. Guo, Y. Fang, D. Wen, L. Wang, J. Yin and S. Dong, *Biosens. Bioelectron.*, 2011, **26**, 1965-1969.

[16] F. Wen, Y. Dong, L. Feng, S. Wang, S. Zhang and X. Zhang, *Anal. Chem.*, 2011, **83**, 1193-1196.

[17] T. Chen, C. Nieh, Y. Shih, C. Ke and W. Tseng, *RSC Adv.*, 2015, **5**, 45158-45164.

[18] H. Deng, G. Wu, Z. Zou, H. Peng, A. Liu, X. Lin, X. Xia and W. Chen, *Chem. Commun.*, 2015, **51**, 7847-7850.

[19] L. Góth, *Clin. Chem. Enzymol. Commun.*, 1989, **1**, 329-331.

[20] W. Chen, L. Hong, A. Liu, J. Liu, X. Lin and X. Xia, *Talanta*, 2012, **99**, 643-648.

[21] T. Chen, Y. Hu, Y. Cen, X. Chu and Y. Lu, *J. Am. Chem. Soc.*, 2013, **135**, 11595-11602.

[22] E. Ju, Z. Liu, Y. Du, Y. Tao, J. Ren and X. Qu, *ACS Nano*, 2014, **8**, 6014-6023.

[23] L. Hu, L. Deng, S. Alsaiari, D. Zhang and N.M. Khashab, *Anal. Chem.*, 2014, **86** 4989-4994.

[24] M. Abbas, W. Luo, L. Zhu, J. Zou and H. Tang, *Food Chem.*, 2010, **120**, 327-331.

[25] A. Georgi, A. Schierz, U. Trommler, C. Horwitz, T. Collins and F.-D. Kopinke, *Appl. Catal. B-Environ.*, 2007, **72**, 26-36.

[26] J. Wei, J. Ren, J. Liu, X. Meng, X. Ren, Z. Chen and F. Tang, *Biosens. Bioelectron.* 2014, **52**, 304-309.

[27] T. Zhang, Y. Lu and G. Luo, *ACS Appl. Mater. Interfaces*, 2014, **6**, 14433-14438.

[28] M.M. Vdovenko, A.S. Demiyanova, K.E. Kopylov and I.Y. Sakharov, *Talanta*, 2014, **125**, 361-365.

[29] Y. Tao, E. Ju, J. Ren and X. Qu, *Chem. Commun.*, 2014, **50**, 3030-3032.

[30] K. Zscharnack, T. Kreisig, A.A. Prasse and T. Zuchner, *Anal. Chim. Acta*, 2014, **834**, 51-57.

[31] X. Xia, Y. Lon and J. Wang, *Anal. Chim. Acta*, 2013, **772**, 81-86.

[32] T. Wen, F. Qu, N. Li and H. Luo, *Anal. Chim. Acta*, 2012, **749**, 56-62.

[33] Y. Ling, N. Zhang, F. Qu, T. Wen, Z. Gao, N. Li and H. Luo, *Spectrochim. Acta Part A Mol. Biomol. Spectrosc.*, 2014, **118**, 315-320.

[34] X. Lv, X. Wang, D. Huang, C. Niu, G. Zeng and Q. Niu, *Talanta*, 2014, **129**, 20-25.

[35] L. Saa and V. Pavlov, *Small*, 2012, **8**, 3449-3455.

[36] S.A. Khan, G.T. Smith, F. Seo and A.K. Ellerbee, *Biosens. Bioelectron.*, 2015, **64**, 30-35.

[37] X. Shan, L. Chai, J. Ma, Z. Qian, J. Chen and H. Feng, *Analyst*, 2014, **139**, 2322-2325.

[38] P. Shen and Y. Xia, *Anal. Chem.*, 2014, **86**, 5323-5329.

[39] Z. Qu, X. Zhou, L. Gu, R. Lan, D. Sun, D. Yu and G. Shi, *Chem. Commun.*, 2013, **49**, 9830-9832.

[40] L. Goth, *Clin. Chim. Acta*, 1991, **196**, 143-151.